Bull. Am. Phys. Soc. 12, 19 (1967), and to be published.
[18]D. J. Horen, Nucl. Data B6(No. 1), 75 (1971).
[19]R. L. Auble and W. H. Kelly, Nucl. Phys. 81, 442 (1966).
[20]P. D. Barnes, private communication.
[21]R. G. Arnold, E. C. Booth, and W. J. Alston, unpublished.
[22]S. Sen and B. R. Sinha, Phys. Letters 31B, 509 (1970).

PHYSICAL REVIEW C VOLUME 7, NUMBER 4 APRIL 1973

Neutron Shell Structure in ^{93}Zr, ^{95}Zr, and ^{97}Zr by (d, p) and $(\alpha, {}^3\mathrm{He})$ Reactions*

C. R. Bingham
The University of Tennessee, Knoxville, Tennessee 37916, and Oak Ridge National Laboratory, Oak Ridge, Tennessee 37830

and

G. T. Fabian†
The University of Tennessee, Knoxville, Tennessee 37916
(Received 12 July 1972)

Differential cross sections for ^{92,94,96}Zr(d,p) at 33.3 MeV were measured in 5° increments from 12.5 to 42.5° lab. The resolution was about 25 keV full width at half maximum. Many levels were characterized which were not reported or were improperly identified in previous neutron-transfer studies. $(\alpha, {}^3\mathrm{He})$ spectra with 55-keV resolution were obtained at 15 and 20° for each target with 65.7-MeV α particles. The data were compared with distorted-wave calculations. With a few exceptions, consistent spectroscopic factors were obtained from the (d,p) and $(\alpha, {}^3\mathrm{He})$ reactions. Sums of spectroscopic factors and centers of gravity are presented for levels assigned to $d_{5/2}$, $s_{1/2}$, $d_{3/2}$, $g_{7/2}$, and $h_{11/2}$ configurations in ^{93}Zr and ^{95}Zr. Except for the $h_{11/2}$ states, these sums are in good agreement with sum-rule predictions. Only ~50% of the expected $h_{11/2}$ strength was observed; the remainder appears to be highly fragmented and at excitation energies above 5 MeV.

I. INTRODUCTION

Earlier spectroscopic results on the neutron shell structure in Zr as obtained from $(\alpha, {}^3\mathrm{He})$ at 65 MeV[1] were not always consistent with results from (d, p) reactions at bombarding energies below 17 MeV.[2-7] As was shown in a recent paper[8] reporting on ^{90,91}Zr(d, p) and ^{90,91}Zr$(\alpha, {}^3\mathrm{He})$ the inconsistencies are largely attributable to unresolved states populated by different l transfers. The resolution for the previous ^{92,94,96}Zr(d, p) experiments[2] was $\gtrsim$75 keV, and that for the $(\alpha, {}^3\mathrm{He})$ experiments was ≈200 keV. As this work was being written up it came to our attention that new experiments on ^{92}Zr(d, p) at 13 MeV are achieving a resolution of 35–45 keV.[9] The present spectrograph experiments were undertaken in order to clarify the neutron structure of ^{93}Zr, ^{95}Zr, and ^{97}Zr, especially for the $g_{7/2}$ and $h_{11/2}$ levels. The higher-l transfers are dominant in the $(\alpha, {}^3\mathrm{He})$ reaction at 65 MeV. However, the angular distributions for $l=4$ and $l=5$ transitions are essentially indistinguishable. To some extent this appears to be true also for (d, p) results at bombarding energies below 15 MeV. In order to enhance the high-l transfers and to make $l=4$ and $l=5$ angular distributions more easily distinguishable, a higher bombarding energy is required. Since optical-model parameters describing the elastic scattering of 34-MeV deuterons[10] and 30- and 40-MeV protons[11] are available, a bombarding energy near 34 MeV was selected. To help clarify the experimental situation, especially with respect to the $l=5$ transfers, spectrograph measurements of the $(\alpha, {}^3\mathrm{He})$ spectra at 65.7 MeV were obtained at 15 and 20°.

II. EXPERIMENTAL DETAILS

The details of the experimental arrangement were given in the previous paper.[8] Briefly, the measurements were made in the spectrograph facility at the Oak Ridge isochronous cyclotron. The protons and ^{3}He were detected in nuclear emulsions which were scanned in $\frac{1}{4}$- and $\frac{1}{2}$-mm strips, respectively.

The thicknesses of the rolled-foil targets were determined by measuring the energy loss of ^{241}Am α particles when penetrating the targets and by interpolation in the range-energy tables of Whaling.[12] The target thicknesses and fractional abundances are given in Table I. The targets were scanned over the α-particle source and were found to be uniform within 10%. This is the principal contribution to the over-all uncertainty of

TABLE I. Target thicknesses and isotopic compositions.

Target	Thickness (mg/cm^2)	Fractional abundances (at.%) ^{90}Zr	^{91}Zr	^{92}Zr	^{94}Zr	^{96}Zr
^{92}Zr	0.77	2.29	0.92	95.7	1.0	0.09
^{94}Zr	0.47	1.67	0.42	0.76	96.93	0.22
^{96}Zr	0.46	9.19	2.02	27.20	4.22	57.36

the absolute cross sections which is estimated to be ±15%.

The ^{92}Zr(d, p) spectrum at 12.5°, shown in Fig. 1, is typical of the (d, p) spectra. Peaks due to other Zr isotopes and light impurities are identified in the figure. Since the isotopic abundance of the ^{96}Zr target was only 57.36%, the background due to impurity peaks was significant and less complete information was obtained for the residual nucleus ^{97}Zr than for the other two. The full width at half maximum of the peaks in the (d, p) spectra was typically 25 keV. The experimental uncertainties on the excitation energies are believed to be about 5 keV for energies below 2 MeV and about 10 keV above 2 MeV.

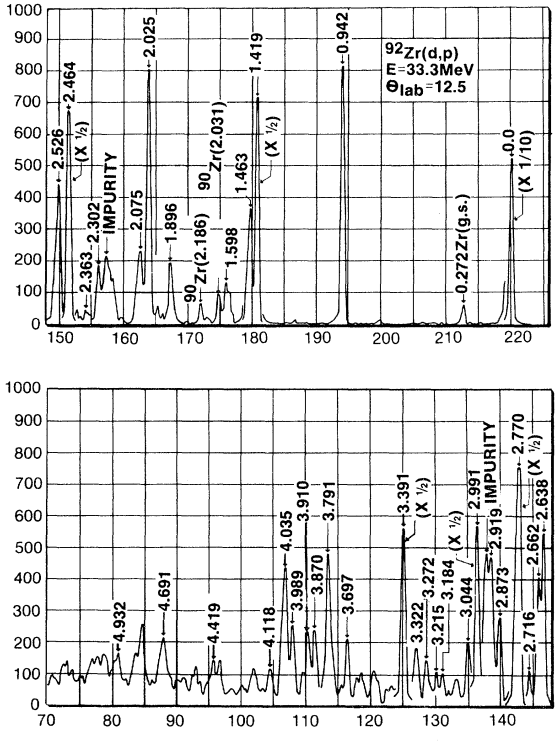

FIG. 1. The ^{92}Zr(d, p) spectrum at 12.5° lab. The excitation energies of the residual states are given for the prominent transitions and peaks from other isotopes identified.

The ^{92}Zr$(\alpha, ^3\text{He})$ spectrum at 15° is shown in Fig. 2. The resolution in this spectrum of about 55 keV is typical of the $(\alpha, ^3\text{He})$ data and hence some of the states resolved in the proton spectra were not resolved here. It is interesting to compare the ^{3}He spectra with the proton spectra for the same residual nuclei. Order-of-magnitude differences in ratios of cross sections for (d, p) and $(\alpha, ^3\text{He})$ are observed. Since the distorted-wave theory predicts these differences, one obtains added confidence in spin assignments by detailed comparison of (d, p) and $(\alpha, ^3\text{He})$ results.

Angular distributions of the proton groups were obtained from 12.5 to 42.5° lab for comparison with distorted-wave predictions. The ^{3}He spectra were obtained at only 15 and 20°, since the $(\alpha, ^3\text{He})$ angular distributions for different l transfers are not easily distinguished.[1]

III. DISTORTED-WAVE ANALYSIS

Distorted-wave calculations were made with the program JULIE[13] for both the (d, p) and $(\alpha, ^3\text{He})$ cross sections. The distorted-wave cross section is given by

$$\frac{d\sigma}{d\Omega} = \frac{NR}{2s+1}\,\frac{2J_f+1}{2J_i+1}\,S\sigma^{(\theta)}_{\text{JULIE}},$$

where J_i and J_f are the spins of the target and residual nuclei, respectively, s $(=\frac{1}{2})$ is the spin of the stripped neutron, S is the spectroscopic factor, and NR accounts for the overlap of the ingoing particle and the outgoing particle-neutron system, as well as the strength of the interaction causing the transition. For the (d, p) calculations a value of $NR = 3.30$ was used as recommended by Satchler.[14] The value of $NR = 92.1$ used here for the $(\alpha, ^3\text{He})$ calculations was obtained empirically in previous work.[15]

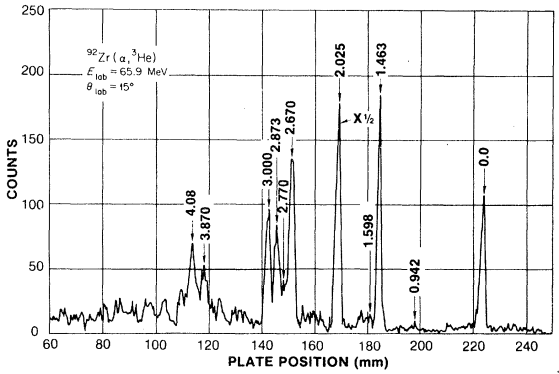

FIG. 2. The ^{92}Zr$(\alpha, ^3\text{He})$ spectrum at 15° lab. The excitation energies of the residual states are given for the prominent transitions.

TABLE II. Optical-model parameters used in the distorted-wave calculations.

Particles	V_0 (MeV)	W_0 (MeV)	W_D (MeV)	V_s (MeV)	r_0 (fm)	a_0 (fm)	r_0' (fm)	a_0' (fm)	r_s (fm)	a_s (fm)	r_c (fm)
^{92}Zr + d	97.92 [a]		12.78	6.17	1.098	0.818	1.28	0.827	r_0	a_0	1.30
^{94}Zr + d	97.74 [a]		15.28	7.00	1.091	0.834	1.25	0.815	r_0	a_0	1.30
^{96}Zr + d	97.92 [a]		15.19	7.50	1.088	0.840	1.245	0.820	r_0	a_0	1.30
^{95}Zr + p	49.9 [b]	5.47	2.83	6.04	1.16	0.75	1.37	0.63	1.064	0.738	1.25
^{3}He	196.9 [c]	17.37			1.04	0.811	1.60	0.797			1.40
^{92}Zr + α	100 [d]	50			1.382	0.662	r_0	a_0			1.40
^{94}Zr + α	100 [d]	53			1.377	0.659	r_0	a_0			1.40
^{96}Zr + α	100 [d]	55			1.377	0.658	r_0	a_0			1.40

[a] Potentials from elastic scattering of 34.4-MeV deuterons, Ref. 10.
[b] Interpolated from potentials of Ref. 11.
[c] Potential A of Ref. 15.
[d] Selected potentials from elastic scattering of 65-MeV α particles, Ref. 18.

The distorted-wave calculation for the (d, p) cross sections employed nonlocal potentials[16] for the ingoing and outgoing channels and finite-range effects in the local energy approximation.[17] No radial cutoffs were used. The ranges used for the deuteron and proton channels were 0.54 and 0.85 fm, respectively. The range of the interaction was taken to be 1.54 fm. The nonlocality and finite-range corrections were made by multiplying the local form factor by appropriate corrective functions.[16,17] The local form factor is the radial bound-state wave function of the stripped neutron. It was taken as the solution of Schrödinger's equation for a Woods-Saxon potential

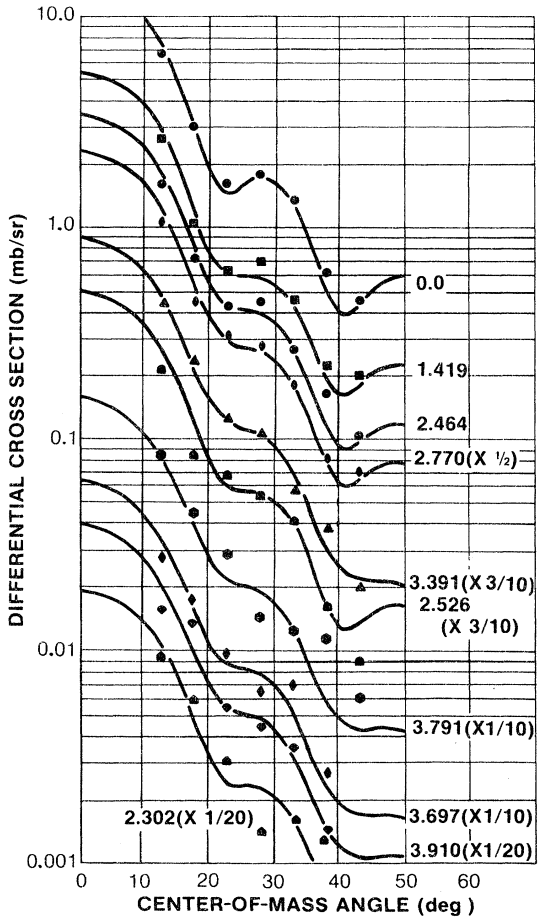

FIG. 3. Experimental angular distributions for $l = 2$ transitions in ^{92}Zr(d, p) (points) in comparison with distorted-wave calculations (smooth curves).

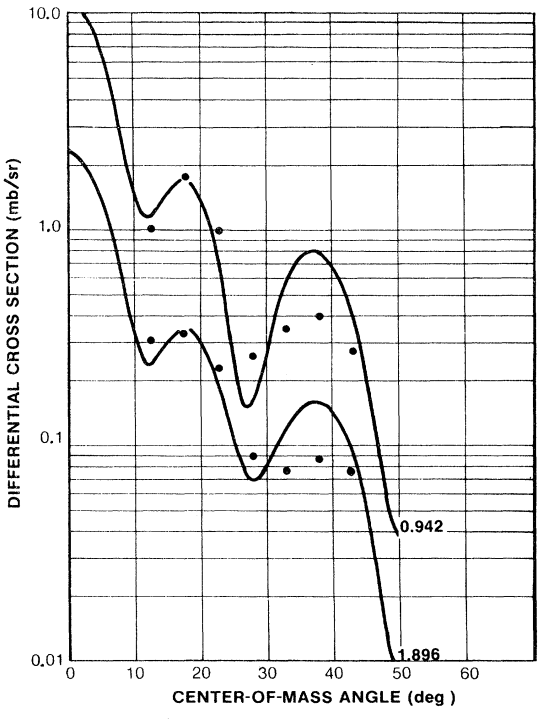

FIG. 4. Experimental angular distributions for $l = 0$ transitions in ^{92}Zr(d, p) (points) in comparison with distorted-wave calculations (smooth curves).

TABLE III. Present results on ^{93}Zr in comparison with ^{92}Zr(d,p) at 15 MeV. A few levels above 4.118 MeV are labeled on Fig. 1, but are not listed here because spins and spectroscopic factors were not obtained. The * indicates a doublet.

Present results					^{92}Zr(d,p) 15 MeV [a]		
E^* (MeV) [b]	nlj	$S_{d,p}$	$S_{\alpha,^3\mathrm{He}}$	S_{adopted}	E^* (MeV)	nlj	S
0.0	$2d_{5/2}$	0.64	0.48	0.56	0.0	$2d_{5/2}$	0.54
(0.272) [c]	$(2d_{3/2})$	~0.004		~0.004	0.28	?	?
0.942	$3s_{1/2}$	0.92		0.92	0.96	$3s_{1/2}$	0.91
1.419	$2d_{3/2}$	0.32	d	0.32	1.45	$2d_{3/2}$	0.38
1.463	$1g_{7/2}$	0.37	0.39	0.38	...	...	...
1.598	$1g_{7/2}$	0.036	0.039	0.037	1.64	$(1g_{7/2})$	0.11
1.896	$3s_{1/2}$	0.23		0.23	1.94	$3s_{1/2}$	0.21
2.025	$1h_{11/2}$	0.22	0.22	0.22			
2.075	$1g_{7/2}$	0.073	d	0.073	2.08	$(1g_{7/2})$	0.42
2.302	$(2d_{3/2})$	0.023		0.023	2.32	$1g_{7/2}$	0.09
2.363	$(1h_{11/2})$	0.011		0.011			
2.464	$2d_{3/2}$	0.20	0.30	0.20	2.50	$2d_{3/2}$	0.24
2.526	$2d_{3/2}$	0.097		0.097			
2.638	$1g_{7/2}$	0.10	d	0.10			
2.662	$1h_{11/2}$	0.08	0.098	0.08			
2.716	$1h_{11/2}$	0.023		0.023			
2.770	$2d_{3/2}$	0.27	0.32	0.29	2.78	$2d_{3/2}$	0.21
2.873	$1h_{11/2}$	0.06	0.042	0.051			
2.919	$(2d_{3/2})$	0.063		0.063			
2.991	$1g_{7/2}$	0.28	0.24	0.26	3.02	$1g_{7/2}$	0.30
3.044	$1g_{7/2}$	0.035		0.035			
3.184	$2d_{3/2}$	0.017		0.017	3.19	$2d_{3/2}$	0.038
3.272	$2d_{3/2}$	0.022		0.022	3.29	$2d_{3/2}$	0.028
3.322	$1g_{7/2}$	0.05	0.035	0.043			
3.391	$2d_{3/2}$	0.17		0.17	3.41	$3p_{3/2}$	0.117
3.697	$2d_{3/2}$	0.037		0.037	3.64*	$(d),(f),(g)$	
3.791	$(2d_{3/2})$	0.11		0.11	3.78*	$3p_{3/2}$, $2d_{3/2}$	0.075, 0.069
3.870	$1h_{11/2}$	0.032	0.042	0.037			
3.910	$(2d_{3/2})$	0.05		0.05			
3.989	$(2d_{3/2})$	0.05		0.05			
4.035	$1g_{7/2}$	0.11	d	0.11	4.03*	$3p_{3/2}$	0.133
4.118	$1h_{11/2}$	0.03	0.046	0.038			
					4.27*	$3p_{3/2}$	0.028
					4.40*	$2d_{3/2}$	0.052
					4.77*	$3p_{3/2}$	0.119
					5.00*	$3p_{3/2}$	0.107

[a] See Ref. 2.

[b] Excitation energies taken from ^{92}Zr(d,p).

[c] Camouflaged by ground state of ^{94}Zr(d,p). The ^{94}Zr in the target accounts for about $\frac{1}{2}$ of the counts observed; hence, this state is somewhat doubtful.

[d] Unresolved from larger peaks in $(\alpha, ^3\mathrm{He})$. The $(\alpha, ^3\mathrm{He})$ cross section was corrected for these unresolved components before analyzing the principal component.

with a spin-orbit term of the Thomas form having $r_0 = 1.24$ fm, $a = 0.65$ fm, $r_{0s} = 1.14$ fm, $a_s = 0.65$ fm, $\lambda = 25$, and a well depth adjusted to give an eigenvalue equal to the binding energy of the transferred neutron.

The wave function for the ingoing deuteron was calculated from a potential which describes the elastic scattering of 34-MeV deuterons from the respective targets.[10] The parameters are listed in the first three lines of Table II.

The proton energies varied from about 32 to 38 MeV. The potential for the proton channel was obtained by interpolation between the potentials which fit the elastic scattering cross section and polarization data at 30 and 40 MeV.[11] The parameters at mid range (~35 MeV) are listed for ^{95}Zr in Table II. The parameters for the other nuclei and energies were very similar.

The $(\alpha, {}^3\mathrm{He})$ calculations, fully described in Ref. 8, were made in zero range with local potentials. The optical-model potentials for α and ^{3}He particles are somewhat ambiguous and effects similar to the effects of nonlocality and finite range can be produced by choosing α potentials with deeper absorptive wells. The ^{3}He potential was obtained from the elastic scattering of 51-MeV ^{3}He from ^{92}Zr.[15] The α potentials used here and listed in Table II were selected from the large number of ambiguous potentials which fit the elastic scattering of 65-MeV α particles from the respective targets.[18] They are similar to those used in previous $(\alpha, {}^3\mathrm{He})$ and $({}^3\mathrm{He}, \alpha)$ analyses[1,15] to fit measured angular distributions.

IV. RESULTS AND DISCUSSION

A. ^{92}Zr Target

The ^{92}Zr(d, p) angular distributions are compared with the distorted-wave predictions in Figs. 3–6. The excitation energies and the spectroscopic factors are given in Table III. Also given in Table III are the spectroscopic factors from $(\alpha, {}^3\mathrm{He})$. The $(\alpha, {}^3\mathrm{He})$ spectroscopic factors agree well with the (d, p) results. The states populated by large l transfers are dominant in the $(\alpha, {}^3\mathrm{He})$ spectra, so that the $l=0$ and small $l=2$ cross sections could not be measured to good accuracy. In cases where neighboring states were not resolved in the ^{3}He spectrum, the contribution due to the lower-l transfer was subtracted and the spectroscopic factor for the higher spin state was then deduced for comparison. The spectroscopic factors adopted in column 5 of Table III are taken in some cases to be the average of the (d, p) and $(\alpha, {}^3\mathrm{He})$ spectroscopic factors; for cases where the $(\alpha, {}^3\mathrm{He})$ transitions are weak, the (d, p) re-

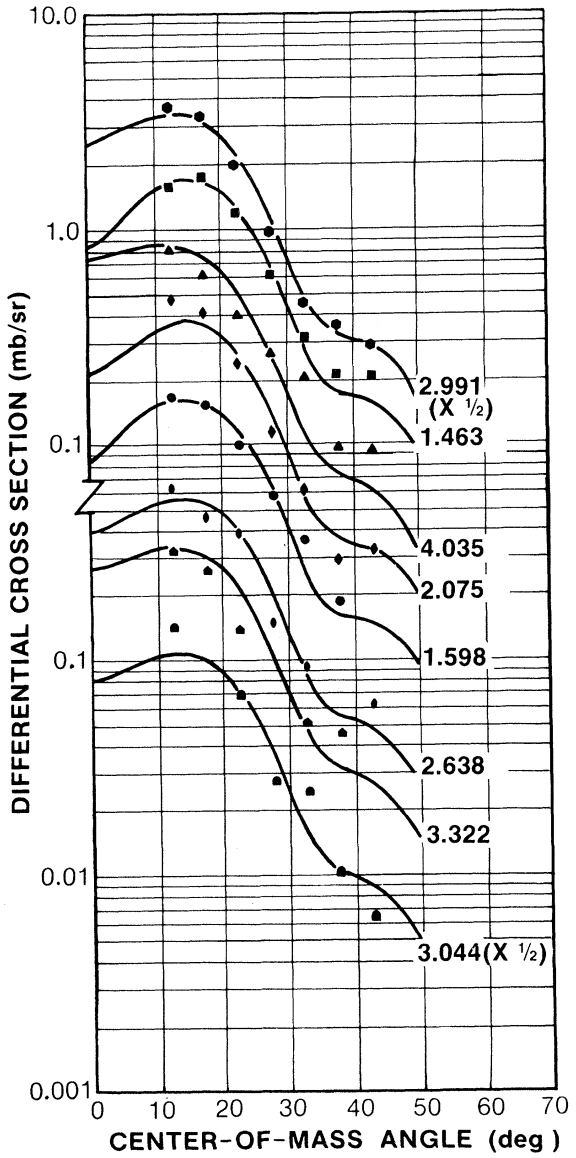

FIG. 5. Experimental angular distributions for $l=4$ transitions in ^{92}Zr(d, p) (points) in comparison with distorted-wave calculations (smooth curves).

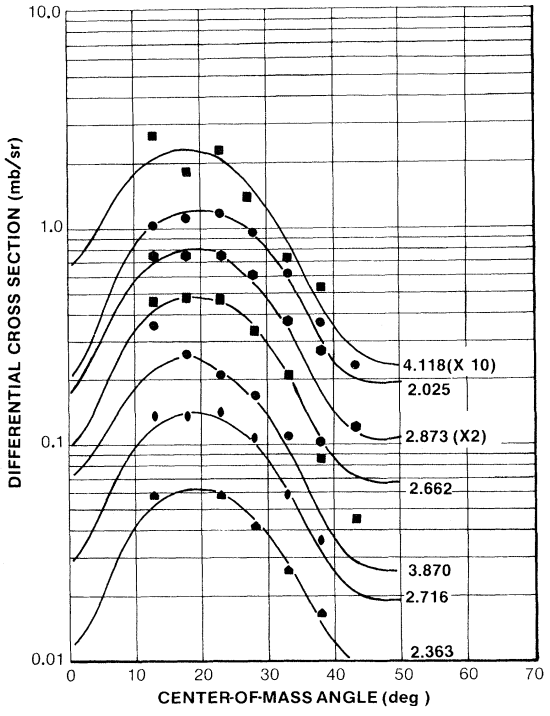

FIG. 6. Experimental angular distributions for $l=5$ transitions in ^{92}Zr(d, p) (points) in comparison with distorted-wave calculations (smooth curves).

sults are adopted.

The ground state is a $\frac{5}{2}^+$ state and is populated by a $2d_{5/2}$ neutron transfer. The spectroscopic factor is close to the theoretically expected value of 0.67. The transition to a possible state at 0.272 MeV was partially concealed by the ^{94}Zr contaminant in the target. Approximately half the counts in the peak can be attributed to the ^{94}Zr abundance. This state is probably primarily composed of three $d_{5/2}$ neutrons coupled to a spin of $\frac{3}{2}$.[19] If the $(d_{5/2})_0{}^2 d_{3/2}$ state mixes with this state then the state could be populated by $d_{3/2}$ transitions. The spectroscopic factor is small indicating that very little mixing occurs. The next $l=2$ transition at 1.419 MeV has a rather large cross section and is, hence, assigned as $d_{3/2}$ as are the higher $l=2$ states. The $l=4$ and $l=5$ transitions are treated as $g_{7/2}$ and $h_{11/2}$ transitions, respectively, since the $g_{9/2}$ shell should be filled[20] and the $h_{9/2}$ shell is expected to lie at much higher energies.

With few exceptions the spectroscopic factors for the $l=0$ and $l=2$ states agree well with those from Ref. 2. In the present work a doublet near 3.5 MeV was resolved and the level near 3.39 MeV was assigned as $d_{3/2}$ rather than $p_{3/2}$ as in Ref. 2. A large $l=4$ level was observed at 1.463 MeV and the ones near 1.60 and 2.08 MeV appear to be much smaller in the present work. The peak for the 2.08-MeV level of Ref. 2 probably included the strong $l=5$ state at 2.025 MeV. The $l=4$ peak at 3.02 MeV was resolved into two $l=4$ peaks in the present experiment and new $l=4$ levels were observed at 2.638, 3.322, and 4.035 MeV. The $l=4$ level reported at 2.32 MeV in Ref. 2 appears to be populated by a possible $l=2$ transition in the present work. None of the seven $h_{11/2}$ states observed here were reported in Ref. 2.

B. ^{94}Zr Target

The angular distributions for ^{94}Zr(d,p) are compared with the distorted-wave predictions in Figs.

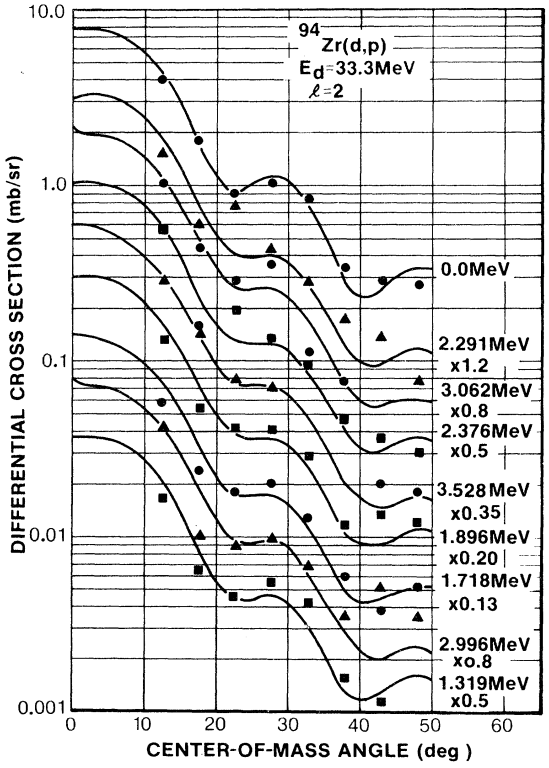

FIG. 7. Experimental angular distributions for $l=2$ transitions in ^{94}Zr(d,p) (points) in comparison with distorted-wave calculations (smooth curves).

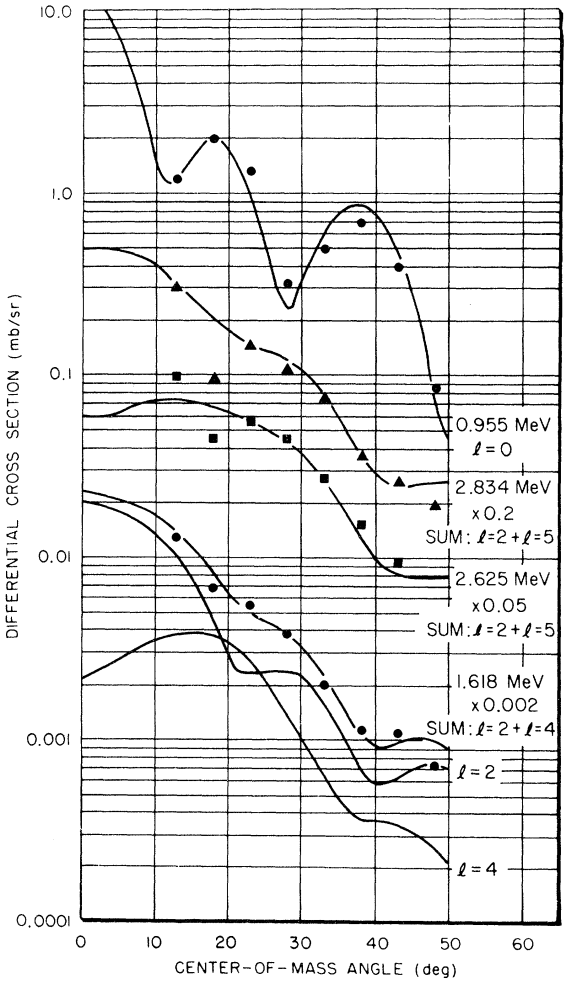

FIG. 8. Experimental angular distributions for the $l=0$ and three doublet transitions in ^{94}Zr(d,p) (points) in comparison with distorted-wave calculations. The $l=2$ and $l=4$ components are shown for the 1.618-MeV transitions.

7–10. The resulting spectroscopic factors are given in Table IV along with those from $(\alpha, {}^3\mathrm{He})$ and the results of $^{94}\mathrm{Zr}(d, p)$ at 15 MeV[2]. The $(\alpha, {}^3\mathrm{He})$ spectroscopic factors appear to be consistently higher than the (d, p) results. The adopted spectroscopic factors given in column 5, Table IV were obtained for the cases where the spectroscopic factors from $(\alpha, {}^3\mathrm{He})$ were measurable by first multiplying $S_{\alpha,{}^3\mathrm{He}}$ by a factor of 0.88 and then averaging the result with $S_{d,p}$; the $S_{d,p}$ were adopted for the other cases.

Three of the peaks had to be treated as doublets in both the (d, p) and $(\alpha, {}^3\mathrm{He})$ spectra in order to obtain consistent spectroscopic factors. The angular distributions for these peaks are shown in Fig. 8 along with the sum of the distorted-wave predictions. The two components are shown for the levels near the 1.618 MeV. In each of these cases the higher-l transition is dominant in the $(\alpha, {}^3\mathrm{He})$ spectrum.

The spectroscopic factor for the $l=0$ transition to the level at 0.955 MeV is in agreement with the result from Ref. 2. However, the $l=0$ levels observed in Ref. 2 near 3.30 and 3.96 MeV were not identified in the present work. The levels are probably camouflaged by stronger transitions in the present work. The results for the $l=2$ transitions are in good agreement, except for the level near 2.291 MeV which was assigned as $2d_{3/2}$ in the present work and as $(3p_{3/2})$ in Ref. 2. The two $d_{3/2}$ levels near 3.0 MeV were not resolved in Ref. 2. The present results for $l=4$ transitions are in agreement with Ref. 2 only for the level at 2.724 MeV. The levels near 2.018 and 3.420 MeV are assigned as $l=5$ transitions rather than $l=4$ as in Ref. 2. A new $l=4$ component was obtained in the peak at 1.618 MeV and the peak at 2.450 MeV is assigned to $l=4$ rather than $l=1$ as in Ref. 2. None of the six $h_{11/2}$ states observed here were previously reported. Several weak $l=1$ and $l=3$ transitions reported in Ref. 2 were not discernible in the present work.

C. ^{96}Zr Target

The angular distributions for the strong transitions in $^{96}\mathrm{Zr}(d, p)$ are compared with the distorted-

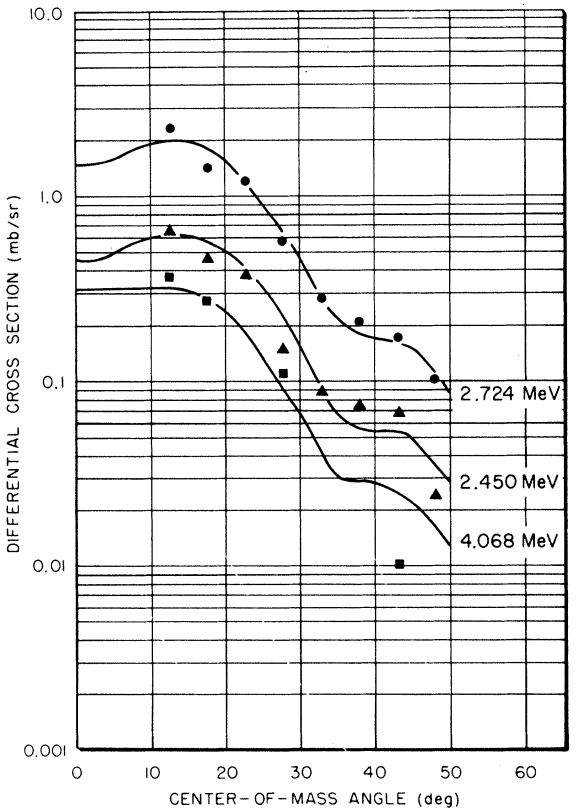

FIG. 9. Experimental angular distributions for $l=4$ transitions in $^{94}\mathrm{Zr}(d, p)$ (points) in comparison with distorted-wave calculations (smooth curves).

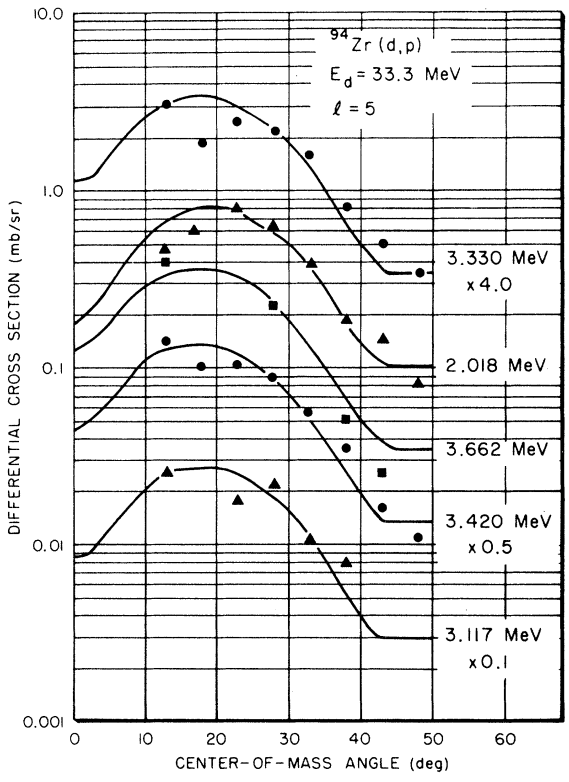

FIG. 10. Experimental angular distributions for $l=5$ transitions in $^{94}\mathrm{Zr}(d, p)$ (points) in comparison with distorted-wave calculations (smooth curves).

TABLE IV. Present results on ^{95}Zr in comparison with ^{94}Zr(d,p) at 15 MeV.

Present results					^{94}Zr(d,p) 15 MeV [a]		
E^* (MeV) [b]	nl_j	$S_{d,p}$	$S_{\alpha,^3\mathrm{He}}$	S_{adopted}	E^* (MeV)	nl_j	S
0.0	$2d_{5/2}$	0.369	0.36	0.34	0.0	$2d_{5/2}$	0.30
0.955	$3s_{1/2}$	1.012	1.09	0.99	0.95	$3s_{1/2}$	0.89
1.319	$2d_{(3/2)}$ [c]	0.044		0.044	1.33	$2d_{3/2}$	0.017
1.618 [d]	$2d_{3/2}$, $1g_{7/2}$	0.54, 0.48	0.54, 0.48	0.54, 0.48	1.64	$2d_{3/2}$	0.45
1.718	$2d_{3/2}$	0.060		0.060	1.73	$2d_{3/2}$	0.05
1.896	$2d_{3/2}$	0.084		0.084	1.91 [d]	$2d_{3/2}$	0.078
2.018	$1h_{11/2}$	0.130	0.179	0.143	2.03	$1g_{7/2}$	0.106
2.291	$2d_{3/2}$	0.148		0.148	2.29	$(3p_{3/2})$	0.124
2.376	$2d_{3/2}$	0.144		0.144	2.40	$2d_{3/2}$	0.080
2.450	$1g_{7/2}$	0.097	0.12	0.101	2.48	$(3p_{3/2})$	0.024
2.625 [d]	$2d_{3/2}$, $1h_{11/2}$	0.050, 0.153	0.050, 0.177	0.050, 0.155	2.65	$(2d_{3/2})$	0.044
2.724	$1g_{7/2}$	0.286	0.39	0.312	2.75	$1g_{7/2}$	0.26
2.834 [d]	$2d_{3/2}$, $1h_{11/2}$	0.123, 0.05	0.123, 0.047	0.123, 0.046	2.87	$2d_{3/2}$	0.099
2.948							
2.996	$2d_{3/2}$	0.044		0.049	3.03 [d]	$2d_{3/2}$	0.093
3.062	$2d_{3/2}$	0.132		0.132			
3.117	$1h_{11/2}$	0.036	0.034	0.033			
3.205					3.23	$2d_{3/2}$	0.027
3.330	$1h_{11/2}$	0.105	0.11	0.101	3.30 [d]	$3s_{1/2}$	0.109
3.420	$1h_{11/2}$	0.033		0.033	3.38	$(1g_{7/2})$	0.039
3.528	$2d_{3/2}$	0.088		0.088	3.54	$2d_{3/2}$, $2f_{7/2}$	0.030, 0.024
3.579							
3.662	$1h_{11/2}$	0.045	0.056	0.047	3.62	$2d_{3/2}$, $2f_{7/2}$	0.030, 0.024
					3.68	$2d_{3/2}$, $2f_{7/2}$	0.016, 0.014
3.810	$1h_{11/2}$		0.076	0.067	3.86	$2d_{3/2}$	0.031
3.855					3.96	$3s_{1/2}$	0.083
4.068	$(1g_{7/2})$	0.035		0.03			

[a] See Ref. 2.
[b] Excitation energies taken from (d,p) results.
[c] Quantities in parentheses are somewhat uncertain.
[d] Indicates doublet.

wave predictions in Figs. 11 and 12. The resulting spectroscopic factors are given in Table V along with those from $(\alpha, ^3\mathrm{He})$ and the results from ^{96}Zr(d,p) at 15 MeV.[2] The spectroscopic factor obtained from ^{96}Zr(d,p) for the ground state exceeds the sum rule by ~20% and $S_{d,p}$ is consistently higher than $S_{\alpha,^3\mathrm{He}}$ by about the same factor. Thus, it is assumed that a systematic error has occurred. The adopted spectroscopic factors were obtained as the average of 0.83 $S_{d,p}$ and $S_{\alpha,^3\mathrm{He}}$ for the cases where $S_{\alpha,^3\mathrm{He}}$ was measured and as 0.83 $S_{d,p}$ otherwise.

The present results agree well with Cohen and Chubinsky[2] for the first four states reported. The $(\alpha, ^3\mathrm{He})$ data require a higher l component in the peak near 1.848 MeV. This component is given a probable $(1g_{7/2})$ assignment. The level near 2.265 is assigned as a $1h_{11/2}$ rather than $1g_{7/2}$ as in Ref. 2. Alternative results are given for the levels at 2.629, 3.014, and 3.652 MeV. The results for the latter two of these states can agree with the lower-energy results[2] for either $d_{3/2}$ or $f_{7/2}$ assignments. Since the peak at 2.629 MeV was not reported in Ref. 2, the $1g_{7/2}$ alternative is probably preferable.

V. SPECTROSCOPIC FACTOR SUMS AND SINGLE-PARTICLE ENERGIES

The spectroscopic factors for each subshell were summed, and the center of gravity of the states in each subshell was calculated with the formula

$$\epsilon = \sum_i E_i^* S_i / \sum_i S_i .$$

These are listed in Table VI for ^{93}Zr, ^{95}Zr, and ^{97}Zr. The ^{97}Zr results are less complete due to

TABLE V. Present results on ^{97}Zr in comparison with ^{96}Zr(d,p) at 15 MeV. The * indicates a doublet.

Present results					^{96}Zr(d,p) 15 MeV [a]		
E^* (MeV) [b]	nlj	$S_{d,p}$	$S_{\alpha,^3\mathrm{He}}$	S_{adopted}	E^* (MeV)	nlj	S
0.0	$3s_{1/2}$	1.197	1.04	1.02	0.0	$3s_{1/2}$	0.98
1.108	$2d_{3/2}$	0.909	0.60	0.68	1.11	$2d_{3/2}$	0.60
1.265	$1g_{7/2}$	0.758	0.57	0.60	1.27	$1g_{7/2}$	0.54
1.399	$2d_{3/2}$	0.108		0.090	1.40	$2d_{3/2}$	0.11
1.848 [c]	$2d_{3/2}$	0.17		0.08 [c]	1.82	$(2d_{3/2})$	0.042
	$(1g_{7/2})$	0.20	0.08	0.08			
					2.07	$(2d_{3/2})$	0.031
2.265	$1h_{11/2}$	0.545	0.48	0.47	2.25	$1g_{7/2}$	0.33
2.629 [d]	$2d_{3/2}$	0.099		0.082 [d]			
	$2f_{7/2}$	0.033		0.027 [d]			
	$1g_{7/2}$	0.081		0.067 [d]			
					2.83	$(3p_{3/2})$	0.08
3.014 [d]	$2d_{3/2}$	0.086		0.072 [d]			
	$2f_{7/2}$	0.031		0.026 [d]			
	$1g_{7/2}$	0.084		0.070 [d]			
					3.05	$2d_{3/2}$	0.046
						$2f_{7/2}$	0.036
					3.16	$3p_{3/2}$	0.04
3.652 [d]	$2d_{3/2}$	0.109		0.091 [d]	3.66	$2d_{3/2}$	0.033
	$2f_{7/2}$	0.036		0.030 [d]		$2f_{7/2}$	0.026
3.731	$1h_{11/2}$	0.126	0.16	0.13	3.76*	$2d_{3/2}$	0.033
						$2f_{7/2}$	0.026
4.586							

[a] See Ref. 2.
[b] Excitation energies taken from ^{96}Zr(d,p).
[c] The peak at 1.848 MeV is treated as a $2d_{3/2}$, $1g_{7/2}$ doublet in order to obtain agreement between (d,p) and $(\alpha, ^3\mathrm{He})$.
[d] The different entries are alternative possibilities for these groups.

TABLE VI. Summary of results for single-particle levels in ^{93}Zr, ^{95}Zr, and ^{97}Zr. The expected spectroscopic factor sums are based on the assumption that the $N=50$ shell is closed and that the lowest energy level results when the remaining neutrons are all in the $2d_{5/2}$ subshell. Values outside parentheses are determined from only states with definite assignments. The numbers inside parentheses are evaluated with all the states that were analyzed including those with some uncertainty.

Residual nucleus	nl_j	Number of transitions	$\sum S_j(i)$ Expected	$\sum S_j(i)$ Measured	ϵ_j (MeV)
^{93}Zr	$2d_{5/2}$	1	0.66	0.56	0.0
	$3s_{1/2}$	2	1.00	1.15	1.13
	$2d_{3/2}$	8(14)	1.00	1.15 (1.45)	2.46 (2.68)
	$1g_{7/2}$	8	1.00	1.04	2.41
	$1h_{11/2}$	6(7)	1.00	0.45 (0.46)	2.59 (2.59)
^{95}Zr	$2d_{5/2}$	1	0.33	0.34	0.0
	$3s_{1/2}$	1	1.00	0.99	0.955
	$2d_{3/2}$	10(11)	1.00	1.39 (1.43)	2.22 (2.20)
	$1g_{7/2}$	3(4)	1.00	0.89 (0.92)	2.11 (2.17)
	$1h_{11/2}$	8	1.00	0.63	2.89
^{97}Zr	$3s_{1/2}$	1	1.00	1.02	0.0
	$2d_{3/2}$	2(6)	1.00	0.77 (1.06)	1.14 (1.68)
	$1g_{7/2}$	1(4)	1.00	0.60 (0.83)	1.26 (1.61)
	$1h_{11/2}$	2	1.00	0.60	2.58

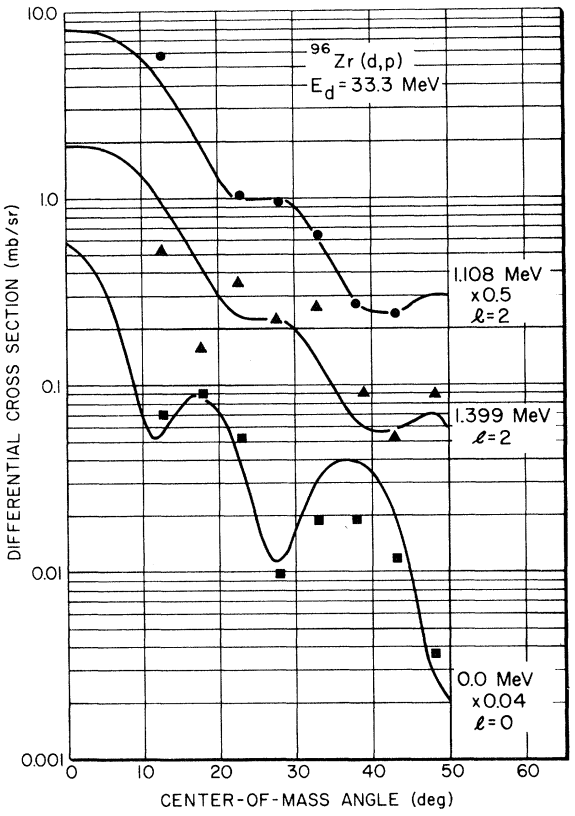

FIG. 11. Experimental angular distributions for $l=0$ and $l=2$ levels in ^{96}Zr(d,p) (points) in comparison with distorted-wave calculations (smooth curves).

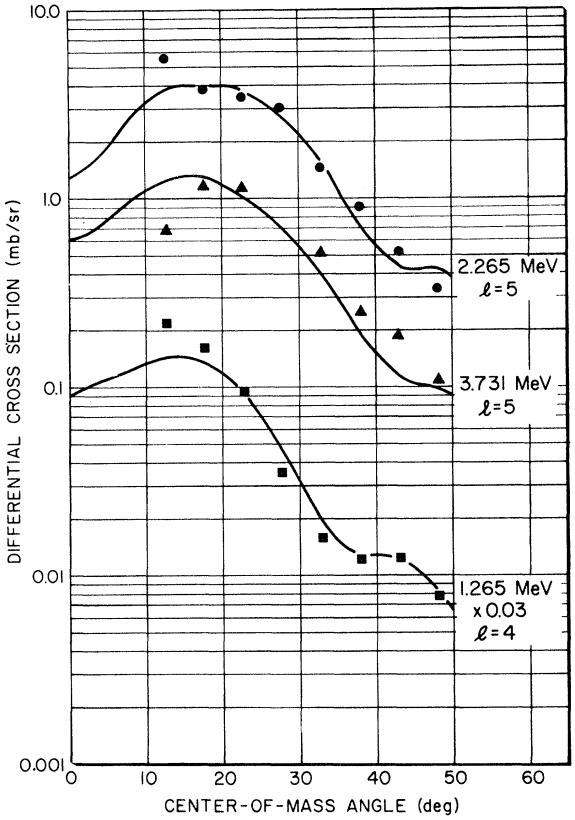

FIG. 12. Experimental angular distributions for $l=4$ and $l=5$ transitions in ^{96}Zr(d,p) (points) in comparison with distorted-wave calculations (smooth curves).

the small isotopic abundance of the target and hence the results are only approximations to the complete picture.

The spectroscopic strengths for the $2d_{5/2}$, $3s_{1/2}$, and $1g_{7/2}$ states agree well with the expected values. The measured spectroscopic strength for the $2d_{3/2}$ states is somewhat higher than expected and that for $1h_{11/2}$ states is ~50–60% of that expected. Similar results were reported previously for ^{91}Zr and ^{92}Zr.[8]

ACKNOWLEDGMENTS

We are indebted to M. L. Halbert and J. B. Ball for many valuable discussions and to M. L. Halbert for his assistance in taking the data. The careful plate scanning of Phyllis Wagner and Barbara Monroe is gratefully acknowledged.

---

*Research supported by the Army Research Office – Durham under a grant to The University of Tennessee and by U. S. Atomic Energy Commission under contract with Union Carbide Corporation.

†Present address: Air Force Weapons Laboratory, Kirtland Air Force Base, Albuquerque, New Mexico 87117.

[1]C. R. Bingham, M. L. Halbert, and R. H. Bassel, Phys. Rev. 148, 1174 (1966).

[2]B. L. Cohen and O. V. Chubinsky, Phys. Rev. 131, 2184 (1963).

[3]C. E. Brient, E. L. Hudspeth, E. M. Bernstein, and W. R. Smith, Phys. Rev. 148, 1221 (1966).

[4]R. L. Preston, H. J. Martin, and M. B. Sampson, Phys. Rev. 121, 1741 (1961).

[5]J. K. Dickens and E. Eichler, Nucl. Phys. A101, 408 (1967).

[6]J. S. Forster, L. L. Green, N. W. Henderson, J. L. Hutton, G. D. Jones, J. F. Sharpey-Schafer, A. G. Craig, and G. A. Stephens, Nucl. Phys. A101, 113 (1967).

[7]G. Simmerstad, M. Iverson, and J. J. Kraushaar, Technical Progress Report, University of Colorado Nu-